URSI GASS 2020, Rome, Italy, 29 August - 5 September 2020

Electron Temperature Prediction by Downshifted Maximum in Stimulated Electromagnetic Emissions via Neural Network

Haiyang Fu*(1), Mingle Jiang(1) , Jian Wu(2), Qingliang Li (2), Michael T. Rietveld(3)
(1) Key Laboratory for Information Science of Electromagnetic Waves (MoE), Fudan University, Shanghai 200433, China
(2) China Research Institute of Radiowave Propagation, Qingdao, China
(3) EISCAT Scientific Association, Ramfjordmoen, Norway

Abstract

High-power high-frequency (HF) radio waves from the ground can generate electromagnetic and electrostatic emission in the ionosphere. The signatures of the electromagnetic emissions observed on the ground are known as Stimulated Electromagnetic Emissions (SEE). The experimental data from recent HF heating experiments near the third electron gyro-frequency ($3f_{ce}$) at EISCAT are presented. The work aims to establish a relation between the spectrum of downshifted maximum (DM) and electron temperature. A neural network architecture is proposed to retrieve electron temperature based on the SEE spectra for the first time. Results show that the neural network can estimate electron temperature using the DM spectral features under certain conditions.

1 Introduction

The interaction between high-power electromagnetic waves and plasmas in the ionosphere can produce stimulated electromagnetic emissions (SEEs), first reported by Thidé et al. [1] and reviewed by Leyser [2]. SEE spectral lines in the scattered wave can be utilized to remotely probe the properties of the ionosphere as well as actively study radio pump-induced phenomenon such as artificial airglow during modification of the ionosphere [3, 4]. Recently, electron temperature determined by SEEs as a complimentary tool of incoherent scatter radar (ISR) have been pursued by many work, including Stimulated Brillouin Scatter (SBS) by Bernhardt[5] at HAARP and SBS by Djuth [6] and Mahmoudian [7] at Arecibo as well as other SEE features by Mahmoudian[8] at EISCAT. The dependence of electron temperature on the SEE spectra is complex and nonlinear, which requires advanced inversion algorithm for plasma parameters. This paper investigates electron temperature measurement based on the SEE spectra automatically with rapid development of artificial intelligence (AI).

2 Experimental Data

The experiment at EISCAT was conducted on November 25, 2019 with the HF transmitter operating at O-mode polarization with full power. The pump frequency was in a range 3.9 MHz $\leq f_0 \leq$ 4.2 MHz through the third harmonic of the $3f_{ce}$. All 12 transmitters on array 2 were used at 80 kW each, resulting in a gain of 22.4 dBi and the effective radiated power (ERP) approximately 148 MW. The beam zenith angle was pointing along the magnetic field line.

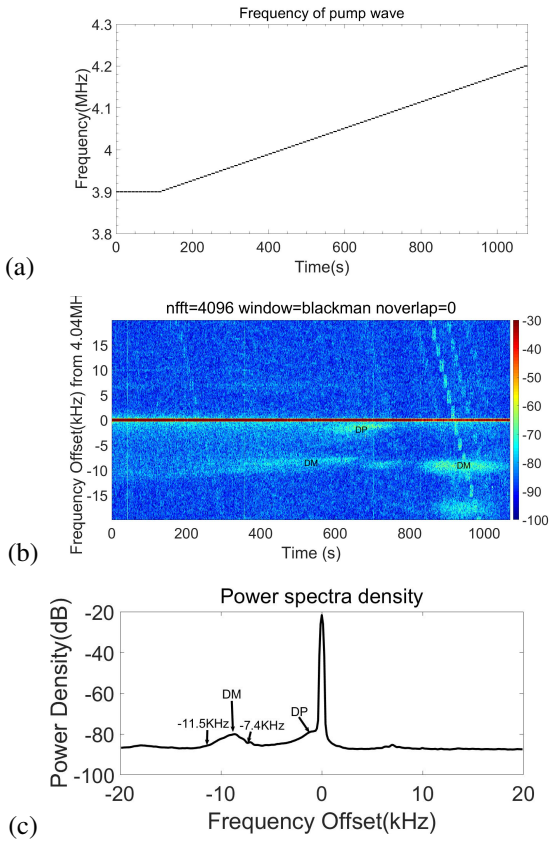

Figure 1. Experimental SEE spectra of scattered waves near $3f_{ce}$ on November 25, 2019 for (a) pump wave frequency (b) 2-D SEE spectrogram and (c) 1-D power spectral density of SEE averaged during the whole cycle.

Figure 1 depicts the time-frequency analysis of scattered electromagnetic waves at UT time 10:45:10∼11:03:10 on November 25, 2019 including (a) the pump wave frequency (b) the SEE spectrum and (c) the power spectra density of SEE. The pump wave frequency is 3.9 MHz between $0 \sim 120$ s, and then increases by 3.125 KHz every 10 s un-

til 4.2 MHz within 1080 s, which corresponds to universal time from UT 10:45:10 to 11:03:10 on November 25, 2019. The spectra in Figure 1b is obtained by short-time Fourier transform (STFT) with frequency resolution is 122 Hz. The DM features appear after 400 s and then is suppressed at 600 $\sim$ 800 s ($f_0 = 4.0701 \sim 4.0703$ MHz) near the $3f_{ce}$. It is also noted that downshifted peak (DP) appears during time 600s$\sim$800s. As shown in Figure 1c, the DM spectrum is at -11.5 KHz ~ -7.4 KHz, and the DP spectrum is at -2 KHz ~ -0.85 KHz.

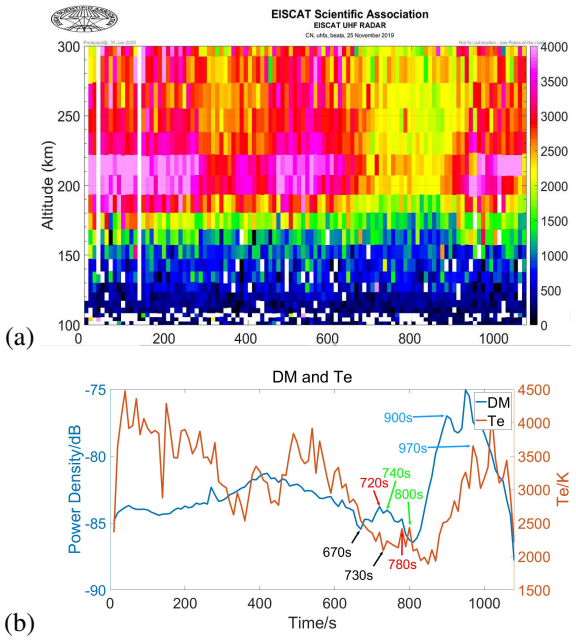

Figure 2. Simultaneous measurement of (a) electron temperature by EISCAT UHF radar and (b) the averaged DM average power and electron temperature in the resonance regimes on November 25, 2019.

Figure 2 shows the electron temperature measured by EISCT UHF incoherent scatter radar and the average power in the DM band of -11.5 KHz ~ -7.4 KHz simultaneously during 10:45:10$\sim$11:03:10 UT on November 25, 2019. The time resolution for electron temperature is 10 s as depicted in Figure 2a. The average power of DM and the average temperature from 186 km to 214 km is shown on the bottom panel of Figure 2b. The relation between DM power and electron temperature are depicted in Figure 2b for pump frequency f_0 from below $3f_{ce}$ to above $3f_{ce}$. As a indicator of pump frequency near $3f_{\rm ce}$, the DP appears at $t \sim 601$s for 4.053 MHz and damps out at $t \sim 740$s for 4.094 MHz. After time $t \sim 600$s, it is noted that that the DM power increased similarly as electron temperature enhancement. However, there seems to exist a delay approximately $\sim$ 60s between DM spectra and electron temperature enhancement. In other words, when the DM power increases, the electron temperature will increase after $\sim$ 60s. As shown by the arrow in figure 2b, the same color arrow indicates the corresponding peak or valley value of electron temperature $T_{\rm e}$ after DM peak or valley. Based on this phenomenon, it enables us to believe that the relationship between DM and electron temperature may be determined by certain models. Therefore, we try to use neural network to build the black box model.

3 Neural Network Model

As neural network has been successfully used in various fields, we aim to investigate the electron temperature inversion based on neural network due to its complexity and nonlinearity. We propose a neural network architecture combining both convolutional neural network (CNN)[9] and recurrent neural network (RNN). We choose CNN as a feature extraction network, which is modified on the basis of AlexNet[10]. Also, RNN is one of the most important machine learning models and have been widely used to perform tasks such as natural language processing [11] and time-series prediction [12, 13]. We also use RNN to take advantage of time characteristics of the DM spectrum during gyro-harmonic heating experiments.

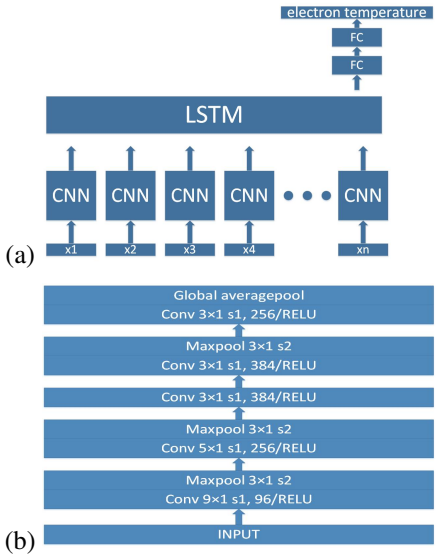

Figure 3. Neural network structure for predicting electron temperature combining CNN, LTSM and fully connected layer (a) with detailed CNN structure as shown in (b).

A neural network architecture is proposed as illustrated in Figure 3. Figure 3a depicts the neural network architecture which combines CNN and RNN. The input DM spectra are listed as $x_1, x_2, .., x_{\rm n}$ at different time. The input spectra are continuously connected with CNN, long short-term memory(LSTM)[14] network and fully connected (FC) layer. We only take the output of the last moment of LSTM as the input of the FC layer. The CNN in Figure 3a represents CNN unit as depicted in Figure 3b. Finally, the network predicts electron temperature as output.

In Figure 3b, it is noted that Conv 9×1 s1, 96/RELU means convolution kernel size 9×1, stride step 1 and the number of convolution kernel 96, and the activation function is RELU. It is worth mentioning that CNN weight sharing. Our CNN design is based on AlexNet. We adjust the size and number of convolution kernels and use the global average

pooling layer instead of the fully connected layer to effectively reduce the number of network parameters and the risk of over-fitting. Compared with AlexNet, this network has fewer parameters, higher classification accuracy and nearly 10 times faster training speed. At the same time, we use more complex LSTM to replace RNN for LSTM's ability to solve the problem of gradient disappearance. Using this network, we train the DM spectrum and make use of time characteristics of DM features for pump frequency with respect to electron gyro-frequency.

4 Result and Analysis

CASE I: the SEE data of $601 \sim 800s$ ($f_0 = 4.0531 \sim 4.1125$MHz, frequency close to $3f_{ce}$) are used for 200s in total. The data are divided into 200 groups, and STFT is carried out respectively. Only the part of frequency between -11.5KHz and -7.4KHz is reserved, and the spectrum feature of each time is extracted by 1-D CNN show in Figure 3b, then input to LSTM according to the time sequence. For training, 90% of DM spectra forms as training set and 10% of them for test. We select training set and test set randomly among 200 groups. The label of each group is the measured electron temperature by UHF incoherent scatter radar. For normalization, we divide electron temperature by a factor of 1429 (1429K is the average temperature of the electron temperature within 20s after the heater is turned off) before putting it into the network.

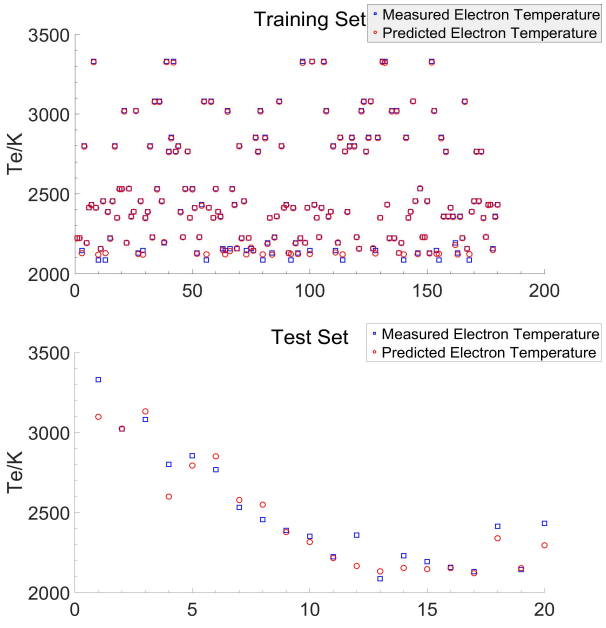

Figure 4. Electron temperature inversion by proposed neural network in comparison with measured data by UHF radar data for CASE I (a) training set and (b) test set.

Figure 4 compares the predicted electron temperature T_e with measured electron temperature by the UHF incoherent scatter radar for case I. Basically, the predicted electron temperature by neural network can agree well with the measured temperature. The root mean square error (RMSE) in training set is 0.0071 and mean relative (MRE) error is 0.26%. The RMSE in test set is 0.0763 and MRE is 2.73%. Test set error is about 10 times of training set error. It is indicated that our network can make good use of DM spectrum to predict electron temperature in the way of training a set of segmentation similar as image classification.

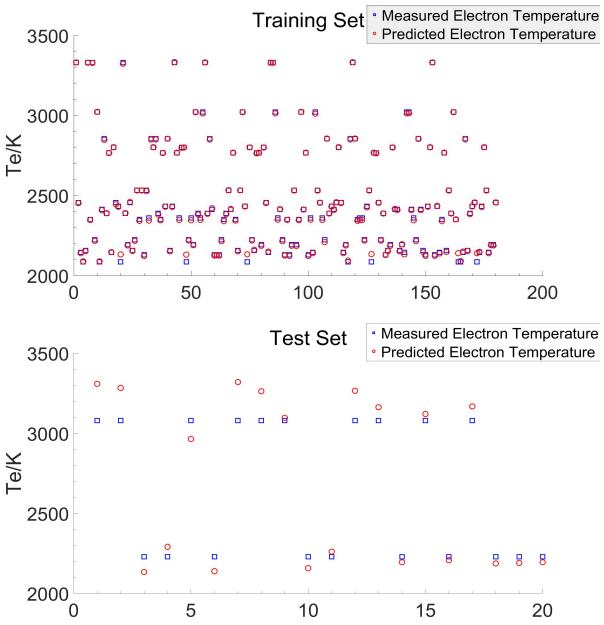

Figure 5. Electron temperature inversion by proposed neural network in comparison with measured data by UHF radar data for CASE II (a) training set and (b) test set.

CASE II: the data and label is as same as CASE I. But we change the way of dividing the training and test group. The pump frequency changes every 10s, so we have 20 frequencies of pump waves. We randomly take the data of two frequencies as the test set and the rest 12 frequencies as the training set. Similar as case I, there are 180 training set data and 20 test data.

Figure 5 compares the predicted electron temperature T_e with measured electron temperature by the UHF incoherent scatter radar for CASE II. The RMSE in training set is 0.0071 and MRE is 0.26%. The RMSE in test set is 0.0852 and MRE is 3.42%. The error of CASE II and CASE I in training set is similar. It is indicated that even if the pump frequency of DM corresponding to the test set does not appear in the training set, the network can still predict the result well with an error of less than 5%. But the error of CASE II in test set is slightly higher than that of CASE I. This is because the difference between test set and training set in CASE II is greater than that in CASE I. In view of this situation, we speculate that if we use other HF heating experimental data, our trained network will not be applicable any more, and many prior conditions may need to be added to use DM spectra to retrieve electron temperature.

Table 1. Inversion error of electron temperature by neural network

	Training set		Test set	
	RMSE	MRE	RMSE	MRE
CASE I	0.0071	0.26%	0.0763	2.73%
CASE II	0.0071	0.26%	0.0852	3.42%

5 Conclusion

In summary, we provide preliminary results of recent experimental SEE campaign at EISCAT and analyze the possible relationship between electron temperature and DM near $3f_{ce}$. Most importantly, we design a neural network to predict electron temperature based on SEE spectral features. The proposed neural network can describe the relation between the DM spectra and electron temperature. The predicted electron temperature by neural network agree with measured electron temperature by ISR radar well.

However, our model, driven by a small amount of data, is likely to be a network that has been fitted for this experiment, and may not be able to be applied to other ionospheric heating experimental data. Therefore, our network can only retrieve electron temperature under certain conditions. In the future, we will consider using more data to train the network and prevent over fitting and try SBS[15] which is associated with electron temperature to carry out experiments to even obtain explicit functional relationship based on the trained network. There is still much work to be done in this future.

6 Acknowledgements

The authors would like to acknowledge staff at the EISCAT facility for technical support and also Tong Xu and Jutao Yang from CRIRP for arranging this campaign. This work is supported by the Shanghai Science and Technology Committee under Grant 19511100600 and Grant 19ZR1403900.

References

[1] B. Thidé, H. Kopka., and P. Stubbe, "Observations of stimulated scattering of a strong high-frequency radio wave in the ionosphere", *Physical Review Letters, 49*,21, 1982, pp. 1561-1564.

[2] T. B. Leyser, " Stimulated electromagnetic emissions by high-frequency electromagnetic pumping of the ionospheric plasma", *Space Science Reviews, 98*,3-4, 2001, pp. 223-328.

[3] T., B. Pedersen, E. Gustavsson, E. Mishin, E. Kendall, T. Mills, H. C. Carlson, and A. L. Snyder, "Creation of artificial ionospheric layers using high-power HF waves", *Geophysical Research Letters, 37*, 2, 2010.

[4] H. Fu, W. Scales, P. Bernhardt, Y. Jin, and S. Briczinski, "Asymmetry in stimulated emission polarization and irregularity evolution during ionospheric electron gyro harmonic heating", *Geophysical Research Letters,* 45, 9363 (2018).

[5] P. A. Bernhardt, C. A. Selcher, R. H. Lehmberg, S. Rodriguez, J. Thomason, M. McCarrick,, and G. Frazer,"Determination of the electron temperature in the modified ionosphere over HAARP using the HF pumped Stimulated Brillouin Scatter (SBS) emission lines", *Annales Geophysicae 27*, 12, 2009, pp. 4409–4427.

[6] Djuth F. T., P. A. Bernhardt, L. Zhang, Magnetized Stimulated Brillioun Scatter Excited in the F region and sporadic E at Arecibo Observatory, Triennial Earth-Sun Summit 20-24 262 May 2018.

[7] Mahmoudian, A., Nossa, E., Isham, B., Bernhardt, P. A., Briczinski, S. J., Sulzer, M.(2019). NSEE yielding electron temperature measurements at the Arecibo Observatory. Journal of Geophysical Research: Space Physics, 124, 3699–3708. https://doi.org/10.1029/2019JA026594

[8] A. Mahmoudian, A. Senior, M. Kosch et al., Investigation of incoherent scatter radar spectra features with stimulated electromagnetic emissions at EISCAT, Advances in Space Research, https://doi.org/10.1016/j.asr.2019.03.028

[9] Lecun Y , Bottou L , Bengio Y, "Gradient-based learning applied to document recognition",*Proceedings of the IEEE*, **86**, 11,1998, pp. 2274–2324

[10] Krizhevsky, Alex and Sutskever, I. and Hinton, G, "ImageNet Classification with Deep Convolutional Neural Networks,"*Advances in neural information processing systems*, **25**, 2,2012

[11] Kaisheng Yao, Geoffrey Zweig, Mei-Yuh Hwang, Yangyang Shi, and Dong Yu, "Recurrent neural networks for language understanding,"*Interspeech*, **23**, 3,2013, pp. 2524–2528

[12] Michael Hsken and Peter Stagge,"Recurrent neural networks for time series classification," *Neurocomputing*, **50**, 2003, pp. 223–235

[13] Georg Dorffner, "Neural Networks for Time Series Processing," *Neural Network World*, **6**, 1996, pp. 447–468

[14] H. Sak, A. Senior, and F. Beaufays, "Long Short-Term Memory Recurrent Neural Network Architectures for Large Scale Acoustic Modeling," *Proc. Interspeech*, 2014

[15] H. Fu*, W. A. Scales, P. A. Bernhardt, S. J. Briczinski, M. J. Kosch, A. Senior, M. T. Rietveld, T. K. Yeoman, and J. M. Ruohoniemi, "Stimulated Brillouin Scattering During Electron Gyro-Harmonic Heating at EISCAT", *Annales Geophysicae*, **33**, 8, 2015, pp. 983–990